Check for updates

Soil water recharge for grassed and forested land covers on the Oak Ridges Moraine, southern Ontario, Canada

R. Bialkowski and J. M. Buttle

ABSTRACT

Soil water recharge (*R*) below 1 m depth was estimated via a 1-d water balance for grasslands, hardwood stands and red pine plantations on the Oak Ridges Moraine (ORM) in southern Ontario, Canada. Annual *R* values (431–696 mm) were in the order of previous estimates for outcropping sands and gravels on the ORM (~400 mm); however, they only partially supported hypothesized differences in *R* between land covers. Annual *R* was similar for grasslands and hardwood stands and exceeded that for red pine plantations. However, there were no consistent differences in *R* between land covers for growing or dormant seasons, due to relatively large uncertainties for *R* estimates as well as inter-site differences in the soil's ability to store and transmit inputs below 1 m. Nevertheless, shifts in annual *R* appear to have accompanied historical land cover changes from hardwood-conifer stands → agricultural fields → red pine plantations → regenerating hardwoods. Growing season *R* in hardwoods makes a larger contribution to total *R* than for other land covers, partly due to spatially focused throughfall and stemflow contributions to *R*. Results highlight the role of land cover differences when assessing spatial variations in *R* along the ORM.

Key words | land cover, reforestation, soil water recharge, stemflow, throughfall, water balance

R. Bialkowski
Environmental and Life Sciences Graduate Program,
Trent University,
Peterborough,
ON K9J 7B8,
Canada

J. M. Buttle (corresponding author)
Department of Geography,
Trent University,
Peterborough,
ON K9J 7B8,
Canada
E-mail: *jbuttle@trentu.ca*

INTRODUCTION

Land cover affects recharge (*R*) through its influence on water delivery to and evapotranspiration (*ET*) from the soil (Healy 2010) and its potential to modify soil properties controlling water storage and transfer (Greenwood & Buttle 2014a). For example, grasslands and forests vary in their interception (*I*), partitioning and use of precipitation and soil water. Reforestation of grasslands increases *I* (Vose *et al.* 2011) and decreases throughfall (*TF*) and snow accumulation (Gelfan *et al.* 2004). Evaporation of intercepted rainfall (Le Maitre *et al.* 1999) and sublimation of intercepted snow (Gelfan *et al.* 2004) in forests is insignificant in grasslands. This, coupled with greater transpiration (Farley *et al.* 2005), leads to enhanced *ET* (Zhang *et al.* 2001; Ladekarl *et al.* 2005) and reduced *R* in forests (Ladekarl *et al.* 2005; Nosetto *et al.* 2005; Wattenbach *et al.* 2007).

Forest composition and age also influence canopy water partitioning, *ET* and *R*. Annual *I* for conifers exceeds that for deciduous species (Houle *et al.* 1999; Barbier *et al.* 2009), reducing water delivery to the soil. This difference is most pronounced in winter when most conifers retain their needles (Pomeroy *et al.* 1998; Houle *et al.* 1999; Komatsu *et al.* 2008), such that snow accumulation and water availability for *R* is greater in deciduous forests (Komatsu *et al.* 2008; LaMalfa & Ryle 2008). Branch architecture influences the spatial distribution of *TF* and stemflow (*SF*), with implications for *R*. Branches sloping toward the tree bole (typical of many deciduous species) promote *TF* focusing close to boles (Carlyle-Moses & Price 2006) and large *SF* fluxes (Voigt 1960). Conversely, trees with branches sloping away from the bole (typical of many conifers) have more uniform sub-canopy *TF* (Loustau *et al.* 1992) or *TF* focusing toward the crown edge (Johnson 1990) along with less *SF* (Barbier *et al.* 2009). Focusing of *TF* and *SF* near deciduous tree boles may enhance *R* via root-induced macropore flow (Johnson & Lehmann 2006). Stand

doi: 10.2166/nh.2015.031

Downloaded from http://iwaponline.com/hr/article-pdf/47/2/390/368866/nh0470390.pdf
by guest

age for a given forest species can affect I and ET with implications for water availability for R. Conifer I may increase with stand age (Bryant *et al.* 2005; Buttle & Farnsworth 2012), and Rosenqvist *et al.* (2010) noted increased I and declining R for ageing Norway spruce stands with no change in either I or R with age for an oak stand.

While hydrological implications of land use changes such as grassland conversion to forest plantations are broadly understood, specific consequences for R are generally unknown despite their important ecological and water resource implications (Scanlon *et al.* 2005; Zhang & Schilling 2006). Such consequences are particularly significant on the Oak Ridges Moraine (ORM) in southern Ontario. This key hydrogeologic feature supplies potable water to many of the region's residents as well as key aquatic ecosystems services (Howard *et al.* 1995; Buttle *et al.* 2015), and accurate R estimates are critical to land use planning in the context of the ORM's groundwater resources (Gerber & Howard 2002). Nevertheless, the influence of land cover on R on the ORM has received relatively little attention (but see Meriano & Eyles 2003). This paper examines point-scale R for major land covers (grasslands, mature mixed hardwood forests and red pine plantations of differing ages) in a managed forest (the Ganaraska Forest, (GF)) on the crest of the ORM by testing the following hypotheses:

1. Annual R will increase in the order old red pine plantation (OP) → young red pine plantation (YP) → mixed hardwoods (MH) → grassland (OPEN), consistent with greater annual I for conifers relative to hardwoods and similar soil ET for all land covers.
2. Dormant season R will increase as in (1) given greater I in pine plantations relative to deciduous stands, whereas growing season R will increase from MH → OP → YP → OPEN, assuming greater growing season I for deciduous species relative to red pines and for OP relative to YP in the GF (Buttle & Farnsworth 2012) and similar ET from the soil for all land covers.

STUDY AREA

The GF (44 °05′N, 78 °30′W; Figure 1) has a hummocky topography (maximum elevation of 384 m asl, relief of 50–70 m) of sand and gravel hills and high ridges comprised of interlayered gravels, sands, silts, clays and minor diamictons (Buttle & Farnsworth 2012). These units rest on Ordovician shale, limestone, dolostone and siltstone bedrock (Gerber & Howard 2002). The regional climate is humid mid-latitude (Köppen Dfb) and mean annual precipitation ranges from ~950 mm on the GF's western edge to ~825 mm on its eastern edge, with ~20% as snow (Greenwood & Buttle 2014a). Mean January and July daily air temperatures are −7.2 °C and 20.5 °C, respectively, and annual ET is ~540 mm (Buttle *et al.* 2014). Annual R on exposed sand and gravel deposits along the ORM is ~400 mm (Gerber & Howard 2000, 2002). Soils are brunisolic grey brown luvisols (sands to sandy loams) of the Pontypool sand and Pontypool gravelly sand series (see Greenwood & Buttle (2014a) and Buttle *et al.* (2014) for more detailed descriptions). The GF is a mosaic of mixed hardwood-conifer stands and red pine ((RP), *Pinus resinosa*) and white pine (*Pinus Strobus*) plantations. Vegetation and forest management practices are described in Buttle *et al.* (2014).

METHODS

Site selection and characterization

Recharge below 1 m depth was estimated at 10 sites from June 23, 2009 to July 12, 2010: two grasslands (OPEN1 – abandoned pasture, OPEN2 – hay field), three mixed hardwood (MH) stands, three young RP (YP) and two old RP (OP) plantations (Figure 1; Table 1). All were on outcropping glaciofluvial sands and gravels on either Pontypool sand or Pontypool gravely sand soils, and were on level ground to minimize potential for lateral water flow. Areas with minimal undergrowth were selected to limit the effects of undergrowth interception and increased permeability associated with undergrowth root networks (Greenwood & Buttle 2014a).

Species, basal area, height, density, leaf area index and canopy density was measured for forest stands (Buttle & Farnsworth 2012; Table 1). Vertical profiles of bulk density, porosity and soil texture were obtained from horizontal cores (6 cm long, 4.8 cm i.d.) at 0.1-m intervals to 1 m from a 1.5 m deep soil pit in the centre of the site, with the exception of OPEN2, YP1 and OP3 where profiles

Downloaded from http://iwaponline.com/hr/article-pdf/47/2/390/368866/nh0470390.pdf
by guest

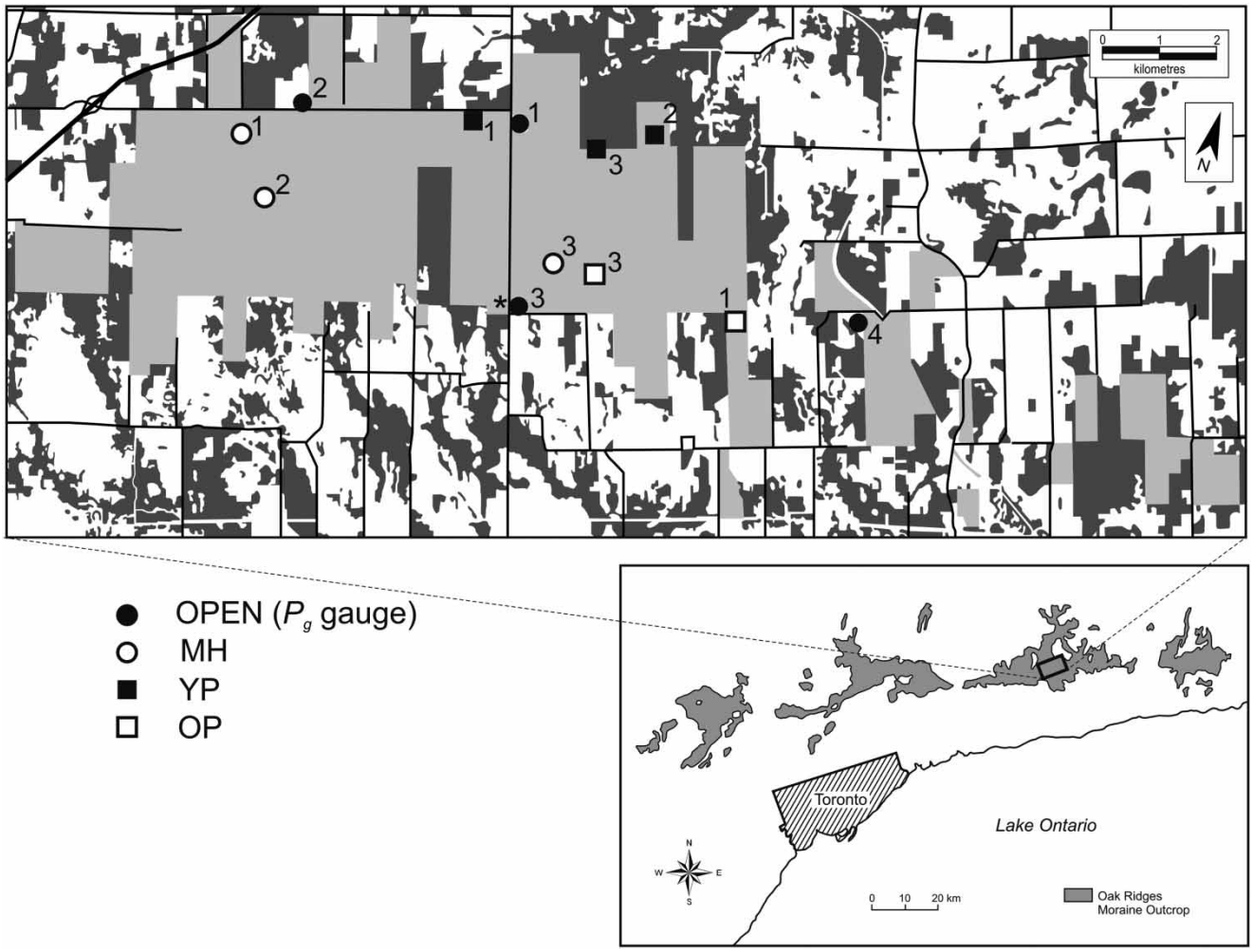

Figure 1 | The Oak Ridges Moraine, Ganaraska Forest (light grey), other forested areas (dark grey), study sites (see Table 1 for details) and rain gauges used to measure above-canopy rainfall (P_g). Air temperature was measured at the P_g site indicated with *.

were from a vertical core to 1 m depth at the centre of the stand and sectioned every 0.1 m. Analytical methods are described in Buttle *et al.* (2014). A single ring infiltrometer and Guelph Permeameter (Reynolds & Elrick 1985) were used to determine saturated hydraulic conductivity (K_H) at the surface and at depth (every 0.1 m to a depth of 0.8 m), respectively.

Precipitation, throughfall, stemflow, snowpack accumulation and melt, and interception

Above-canopy precipitation (P_g) was measured at OPEN1 and OPEN2 and at two other clearings with a standard rain gauge (Figure 1) while *TF* was the average catch of 10 randomly sited rain gauges in each forest site (Buttle & Farnsworth 2012). Ten MH trees at MH1 and four RP trees at both YP1 and OP3 (Table 2) were used to estimate *SF* as described by Buttle *et al.* (2014). All *SF* infiltrated the soil within ~0.2 m of the bole (Buttle *et al.* 2014); thus, *SF* volume was divided by the area of a 0.2 m wide ring around each bole to obtain *SF* depth (mm). Measurements of *TF* and *SF* were not made during winter due to the inability to regularly access some sites, and *SF* was assumed to be negligible.

Snowpack depth, density and snow water equivalent (*SWE*) were periodically measured using a Meteorological Service of Canada (MSC) snow tube along a 12-point snow course at OPEN1 and OPEN2, and at three locations

Downloaded from http://iwaponline.com/hr/article-pdf/47/2/390/368866/nh0470390.pdf
by guest

Table 1 | Site characteristics

Study site	Year planted	Trees ha^{-1}	Basal area (m^2 ha^{-1})	Mean canopy density (%)	Red pine (%)	White oak (%)	Sugar maple (%)	American beech (%)	Long grass (%)
MH1	NA	775	32.2	23–91	6.4	35.5	48.4	9.7	0
MH2	NA	825	42	21–93	0	51.5	33.3	15.2	0
MH3	NA	1150	32.4	23–93	0	50	41.3	8.7	0
YP1	1981	1550	26.9	68.3	100	0	0	0	0
YP2	1981	1275	26.3	77.9	100	0	0	0	0
YP3	1983	1500	39.2	78.3	100	0	0	0	0
OP1	1948	525	35	86.2	100	0	0	0	0
OP3	1947	450	37.5	82.2	100	0	0	0	0
OPEN1	NA	0	0	0	0	0	0	0	100
OPEN2	NA	0	0	0	0	0	0	0	100

The range in the MH sites' mean canopy density represents the leaf-off (minimum) and leaf-on (maximum) extremes.
NA, data not available.

Table 2 | Characteristics of trees used to measure stemflow (*SF*)

MH1						YP1		OP3	
Species	DBH (m)	PCA (m^2)	Species	DBH (m)	PCA (m^2)	DBH (m)	PCA (m^2)	DBH (m)	PCA (m^2)
O	0.45	101.2	SM	0.35	60.6	0.14	3.0	0.25	18.3
O	0.12	16.5	SM	0.09	8.2	0.13	2.8	0.29	20.3
WA	0.25	47.0	B	0.12	6.8	0.08	3.2	0.36	22.2
WA	0.32	52.6	B	0.15	14.6	0.20	7.2	0.43	39.2
SM	0.48	163.9	B	0.11	10.3				
SM	0.22	40.7	B	0.14	42.8				

O is white oak, *WA* is white ash, *SM* is sugar maple and *B* is American beech. All trees sampled at YP1 and OP3 were red pines.
DBH, diameter at breast height; PCA, projected canopy area.

(spacing of ~6 m) along each cardinal direction from a centrally located tree in each forest site. Regressions of spring, summer and fall P_g and *TF* from OPEN and RP sites against P_g at the nearest MSC climate station (Tapley, ~10 km north of the GF) were used to estimate winter rainfall (P_r) and *TF* as rain (TF_r) at these sites. At MH sites TF_r was equated to P_r at the nearest OPEN site since *I* at MH sites was assumed to be 0 during the leaf-off period. All TF_r and P_r was assumed to bypass the snowpack and be input directly to the soil. Throughfall as snow (TF_s) at each site was equal to snowfall at Tapley, with YP and OP inputs adjusted to reflect *I* (see below). Snowmelt was estimated from:

$$\text{melt (mm)} = TF_s - \Delta S_{snowpack} \quad (1)$$

where $\Delta S_{snowpack}$ is changed in *SWE* between successive snow surveys. Negative melt values from Equation (1) produced by an increase in *SWE* in excess of TF_s during that period were set to 0.

Interception at OPEN sites was assumed to be 0 due to lack of tree cover. Spring, summer and fall *I* for each forest stand was:

$$I = P_g - (TF + SF) \quad (2)$$

where P_g was from the nearest clearing. Stand-scale *SF* was estimated by expressing total *SF* volume in a given stand type relative to basal area (m^2) of the sampled trees and up-scaling by basal area (m^2 ha^{-1}) of the stands of that

Downloaded from http://iwaponline.com/hr/article-pdf/47/2/390/368866/nh0470390.pdf
by guest

type. Winter I was assumed to be 0 at MH sites, and was calculated for RP sites as:

$$I = I_r + I_s \tag{3}$$

where I_r and I_s are rainfall and snowfall I, respectively. The former was estimated using Equation (2), while I_s was the difference in SWE between OPEN1 and each RP site.

Soil water content

Soil water content (SWC, $m^3\ m^{-3}$) was measured with a calibrated Delta T PR2/6 Profile Probe™ at 0.1, 0.2, 0.3, 0.4, 0.6 and 1 m depths in ATL-1 access tubes installed at each site 1.1 m from the nearest tree bole, as described in Buttle *et al.* (2014). Soil water storage in the upper 1 m of soil on day t (S_t, mm) was:

$$S_t = \sum_{i=1}^{m} (SWC_i z_i) \tag{4}$$

where SWC_i is soil water content at the midpoint of soil layer i with a thickness z_i (mm). Temporal changes in S_t (ΔS_t, mm) were:

$$\Delta S_t = S_t - S_0 \tag{5}$$

where S_0 is initial depth (June 23, 2009). Values of ΔS_t significantly different from 0 ($P = 0.05$) were determined using Z-scores (Winkler & Hays 1975):

$$Z = \frac{S_t - S_0}{\sqrt{\sigma {S_t}^2 + \sigma {S_0}^2}} \tag{6}$$

where σS is error in S at the respective time:

$$\sigma S = \sqrt{\sum_{i=1}^{m} (\sigma_i^2)} \tag{7}$$

and

$$\sigma_i = (SWC_i z_i) \times 0.15 \tag{8}$$

where 0.15 is the average SWC range about the calibration relationship in Buttle *et al.* (2014). Non-significant ΔS_t values from Equation (6) were set to 0; otherwise ΔS_t was determined from Equation (5).

Evapotranspiration

Above-canopy ET in 2009 was from the MOD16 global ET product (Mu *et al.* 2011), which simulates spatially distributed 8-day ET at 1 km^2 resolution. The MOD16 grid was overlain on LANDSAT 7 imagery to identify pixels that best represented each land cover, and pixels composed predominantly of a single land cover were selected to minimize convolution from mixed pixels. One pixel was used for MH while two pixels were averaged for OPEN ET. Nine pixels covering a 3×3 km area and dominated by RP were examined. Young or old RP or white pine stands could not be differentiated, so pixels likely contained a mix of the three types. Pixels with total ET in $2009 > 1$ standard deviation above the mean were excluded as outliers, and 8-day ET values for remaining pixels were averaged to estimate ET for YP and OP stands. Estimates were divided by eight to obtain daily ET. Canopy I was subtracted from MOD16 ET to estimate direct soil evaporation plus transpiration. MOD16 data were unavailable for 2010, and regression relationships between 2009 MOD16 ET for the land covers and 2009 potential ET from the Hamon model (Dingman 2002) were used to predict 2010 ET. Temperature data for ET estimation were obtained from a BML-TS-7 Thermilinear Air Temperature Sensor at a clearing used to measure P_g (Figure 1).

Recharge

Cumulative R was estimated for a 384-day period subdivided into growing season, fall and winter–spring. Growing season was June 23–October 1, 2009 and May 5–July 12, 2010. The fall period was October 2–December 4, 2009 (decreasing MH leaf area index and ET for all land cover), while winter–spring was December 5, 2009–May 4, 2010 (MH leaf area index approaching its maximum). Recharge was estimated for snow-free and snow-covered conditions.

Downloaded from http://iwaponline.com/hr/article-pdf/47/2/390/368866/nh0470390.pdf
by guest

Cumulative OPEN R at time t (R_t) for snow-free conditions was estimated as:

$$R_t = \left(\sum_{t=0}^{n} [P_{gt} - ET_t]\right) - \Delta S_t \quad (9)$$

P_g and ET are summed from day 0 (June 23, 2009) to measurement day t, with ΔS_t from Equation (5). Bialkowski & Buttle (2015) showed that branch architecture in MH1 focused SF within ~0.2 m of the bole as well as greater TF within ~0.5 m of the bole relative to distal locations. In RP sites TF did not vary with distance from the bole but there was minor focusing of SF within ~0.2 m of the bole. Thus, cumulative forest R at time t was:

$$R_t = aR_{0.2_t} + bR_{0.5_t} + cR_{R_t} \quad (10)$$

where $R_{0.2}$ is R within 0.2 m of the boles, $R_{0.5}$ is from 0.2 to 0.5 m of the boles, R_R is for the remaining forest area, and a, b and c are weighting factors. $R_{0.2}$, $R_{0.5}$ and R_R were calculated as:

$$R_{0.2_t} = \left(\sum_{t=0}^{n} [TF_{F_t} + SF_t - \{ET_t - I_t\}]\right) - \Delta S_t \quad (11)$$

$$R_{0.5_t} = \left(\sum_{t=0}^{n} [TF_{F_t} - \{ET_t - I_t\}]\right) - \Delta S_t \quad (12)$$

$$R_{R_t} = \left(\sum_{t=0}^{n} [\overline{TF}_t - \{ET_t - I_t\}]\right) - \Delta S_t \quad (13)$$

where TF_F is focused TF and $\overline{TF}$ is average catch from the 10 TF gauges in each stand. In MH stands TF_F was estimated from regression of average TF for the two MH1 TF gauges nearest the bole (0.1 and 0.3 m; Bialkowski & Buttle 2015) and $\overline{TF}$ (Figure 2). There was no adjustment to TF beyond 0.5 m. Equations (11)–(13) assume evaporation of I before ET from the soil occurred. If I exceeded above-canopy ET for a given sampling interval, residual I was carried over to the next interval.

Basal area was estimated in two or three 314 m^2 circular plots in each stand, and the 0.2 and 0.2–0.5 m focusing zones areas around each tree were calculated. Weighting factors a and b ranged from 0.012 to 0.022 and 0.036 to 0.073 in MH stands, respectively, while a ranged from 0.012 to 0.063 in RP stands ($b = 0$ given no focused TF).

Recharge under snow-covered conditions was:

$$R_t = \left(\sum_{t=0}^{n} [TF_{r_t} + \mathrm{melt_t} - \{ET_t - I_t\}]\right) - \Delta S_t \quad (14)$$

with $I = 0$ at OPEN and MH sites. Recharge values and associated errors (from Bialkowski 2015) were used in Z-scores to assess the statistical significance of differences in R and $R{:}P_g$ between land covers.

RESULTS

Soil properties

Sites did not show systematic differences in porosity (Figure 3) or K_H (Figure 4), although some (e.g., MH1) had marked variations in K_H with depth (Figure 4). There were pronounced inter-site differences in soil texture (Figure 5), despite site location on either Pontypool sand or Pontypool gravelly sand. Sand dominated all sites and clay was a minor constituent, with the exception of OPEN2 which was largely silt. MH sites had large gravel contents and marked textural variation with depth.

Precipitation, throughfall, stemflow, snowmelt and interception

Total P_g for July 1, 2009–June 30, 2010 (1,199–1,335 mm, Table 3) was well above the 840 mm annual average at Peterborough Airport (Environment Canada 2011) ~30 km to the northeast. Total snowfall for the 2009–2010 winter was 82 cm at Tapley, approximately half the normal depth. Mean TF as a fraction of P_g was similar between forest sites (0.8–0.87); however, MH $TF{:}P_g$ ratios increased when TF focusing near the bole was considered. MH $TF{:}P_g$ ratios increased between the growing season and winter–spring; conversely, $TF{:}P_g$ for YP and OP generally decreased between these periods, reflecting greater snow interception efficiency. MH stands generated more SF than either YP

Downloaded from http://iwaponline.com/hr/article-pdf/47/2/390/368866/nh0470390.pdf
by guest

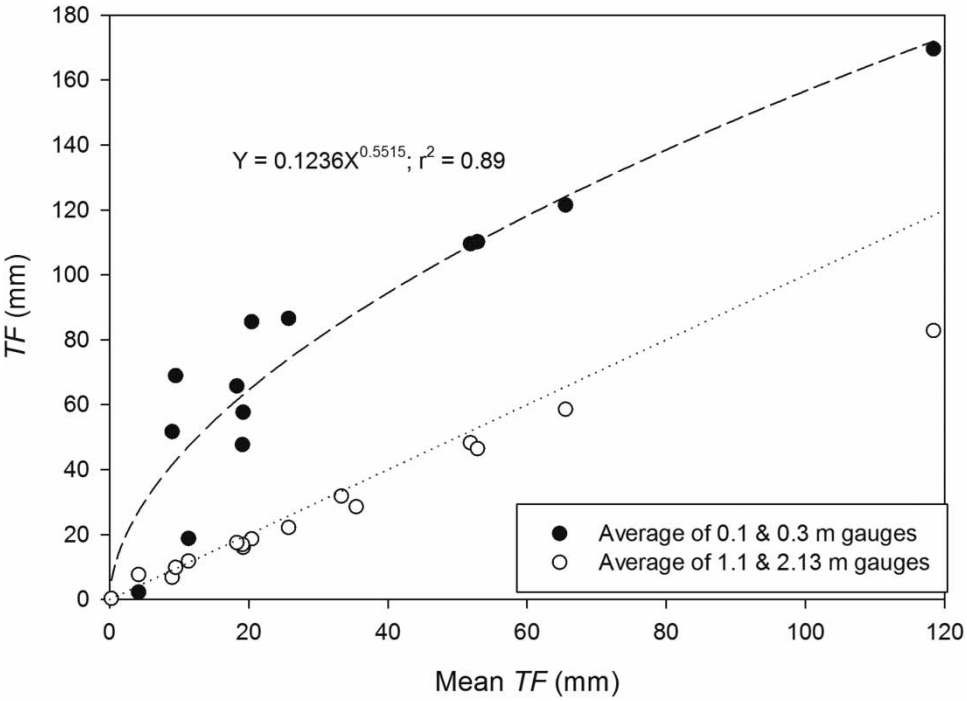

Figure 2 | Mean *TF* from two proximal (0.1 and 0.3 m) and distal (1.10 and 2.13 m) *TF* gauges from the tree bole in MH1 (from Bialkowski & Buttle 2015) vs. mean catch of 10 *TF* gauges in MH1. Dotted line is 1:1 relationship and dashed line is regression relationship between mean *TF* from the two most proximal *TF* gauges and mean stand *TF*.

or OP, whether *SF* was expressed relative to stand area or the 0.2 m wide focusing zone adjacent to the bole. Both *TF* focused within 0.5 m of the bole and *SF* focused within 0.2 m of the bole exceeded P_g for MH stands.

Maximum *SWE* for all but one site (OPEN2) occurred at the beginning of March 2010. Snowmelt ended by March 18, 2010 with the exception of MH2 where it ended a week later. OPEN and MH sites generally had more *SWE* than RP sites (peak *SWE* of 95–125 mm at the former vs. 48–90 mm at the latter), with least *SWE* at OP sites. Differences in peak *SWE* for RP relative to OPEN sites suggest I_s between 25 and 40% of P_g.

Period *I* ranged from 159 mm (YP3) to 260 mm (OP3), representing 13% and 19% of P_g, respectively (Table 3). Mean MH, YP and OP *I* for the study period was 220 ± 31 mm, 177 ± 30 mm and 227 ± 47 mm, respectively.

Soil water storage

Soil water storage at each site (Figure 6) was estimated from a single access tube. Changes in S_t at the access tube 1.1 m from the bole were correlated ($P < 0.05$) with ΔS_t integrated along access tube transects extending ~2 m from tree boles at MH1, YP1 and OP3 (Bialkowski & Buttle 2015). This suggests that the single tube provided a good representation of ΔS_t at each site. All sites showed minimum S_t during the growing season, increasing S_t with fall wetting-up, declining S_t during winter, wetting-up during snowmelt, and subsequent drainage (Figure 6). Inter-site differences in S_t response to wetting-up and drainage were pronounced, with OPEN1, OPEN2, MH3, YP2 and YP3 showing greater temporal variability than the remaining sites. The range in S_t was 119 mm (OPEN2) to 211 mm (OPEN1) at the former, but 47 mm (MH1) to 85 mm (YP1) at the latter. These differences may partly reflect soil texture, with greatest S_t at OPEN2 with its silty soil and smallest S_t at MH2 with large gravel contents at depth (Figure 5). However, soil properties could not explain differences in temporal patterns of S_t at other sites.

Evapotranspiration

Total period above-canopy *ET* (Figure 7) ranged from 586 mm (OPEN sites) to 701 mm (RP stands), with

Downloaded from http://iwaponline.com/hr/article-pdf/47/2/390/368866/nh0470390.pdf
by guest

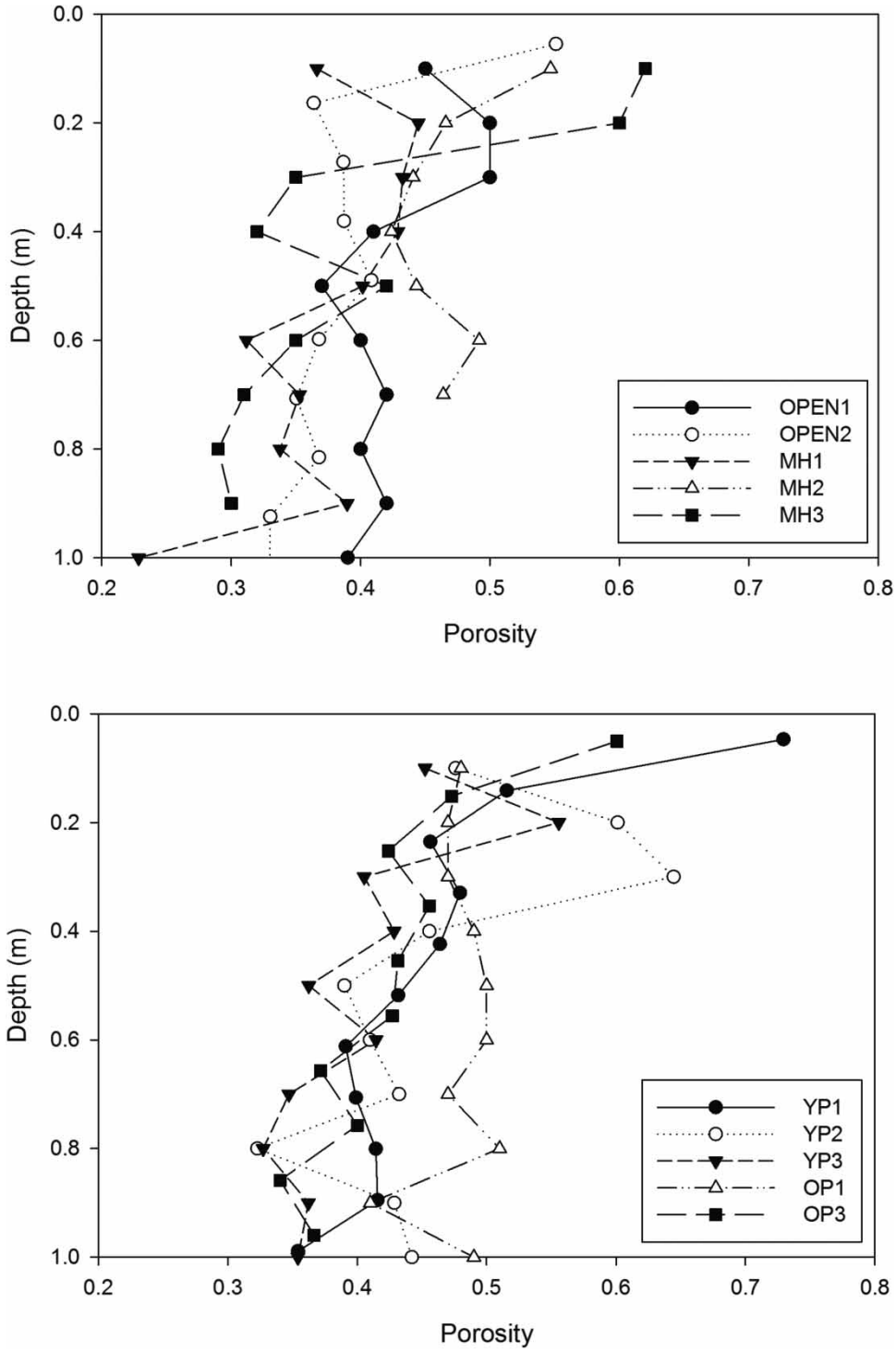

Figure 3 | Vertical profiles of soil porosity.

maximum daily *ET* of 3.2 (OPEN), 4.4 (MH) and 4.0 (RP) mm d^{-1}. Ratios of $ET{:}P_g$ ranged from 0.47 (MH3) to 0.58 (OP1). Removal of *I* from *ET* for forest sites reduced *ET* from the soil relative to OPEN sites. Soil *ET* for YP (530–550 mm) and OP (467–488 mm) stands exceeded MH values (362–427 mm).

Downloaded from http://iwaponline.com/hr/article-pdf/47/2/390/368866/nh0470390.pdf
by guest

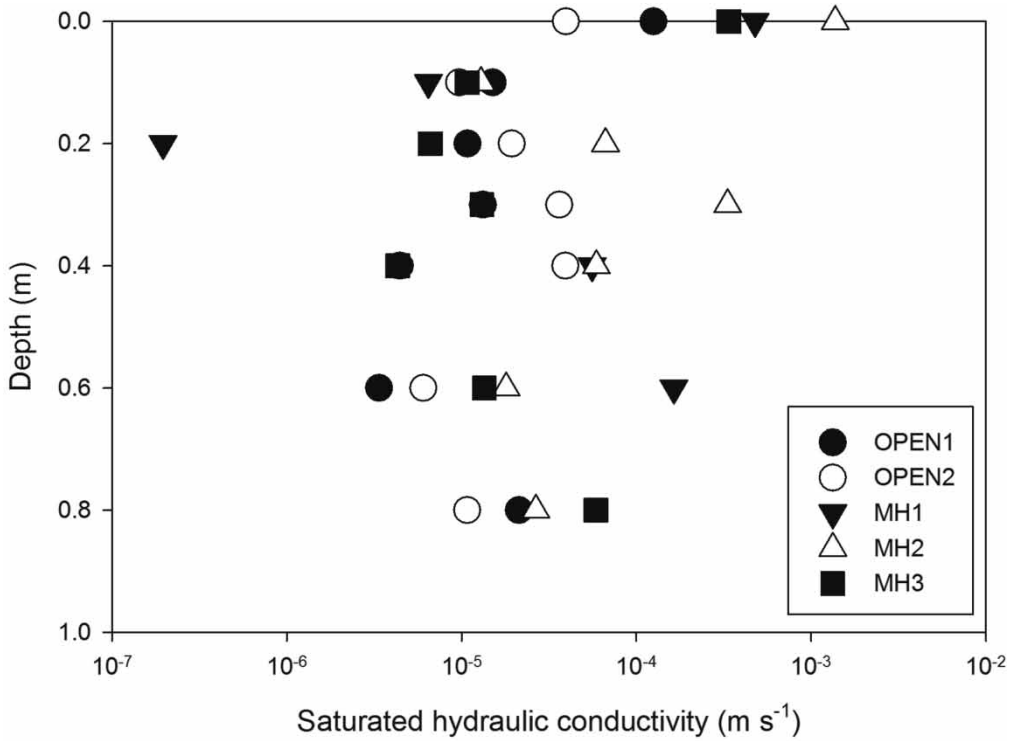

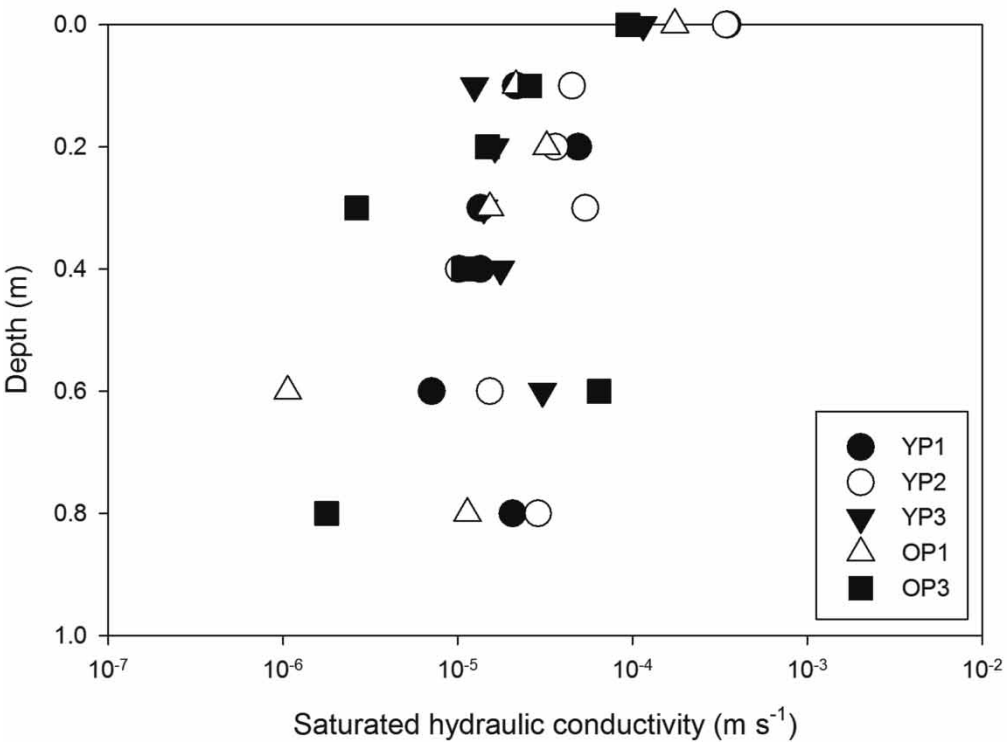

Figure 4 | Vertical profiles of saturated hydraulic conductivity (K_H).

Downloaded from http://iwaponline.com/hr/article-pdf/47/2/390/368866/nh0470390.pdf
by guest

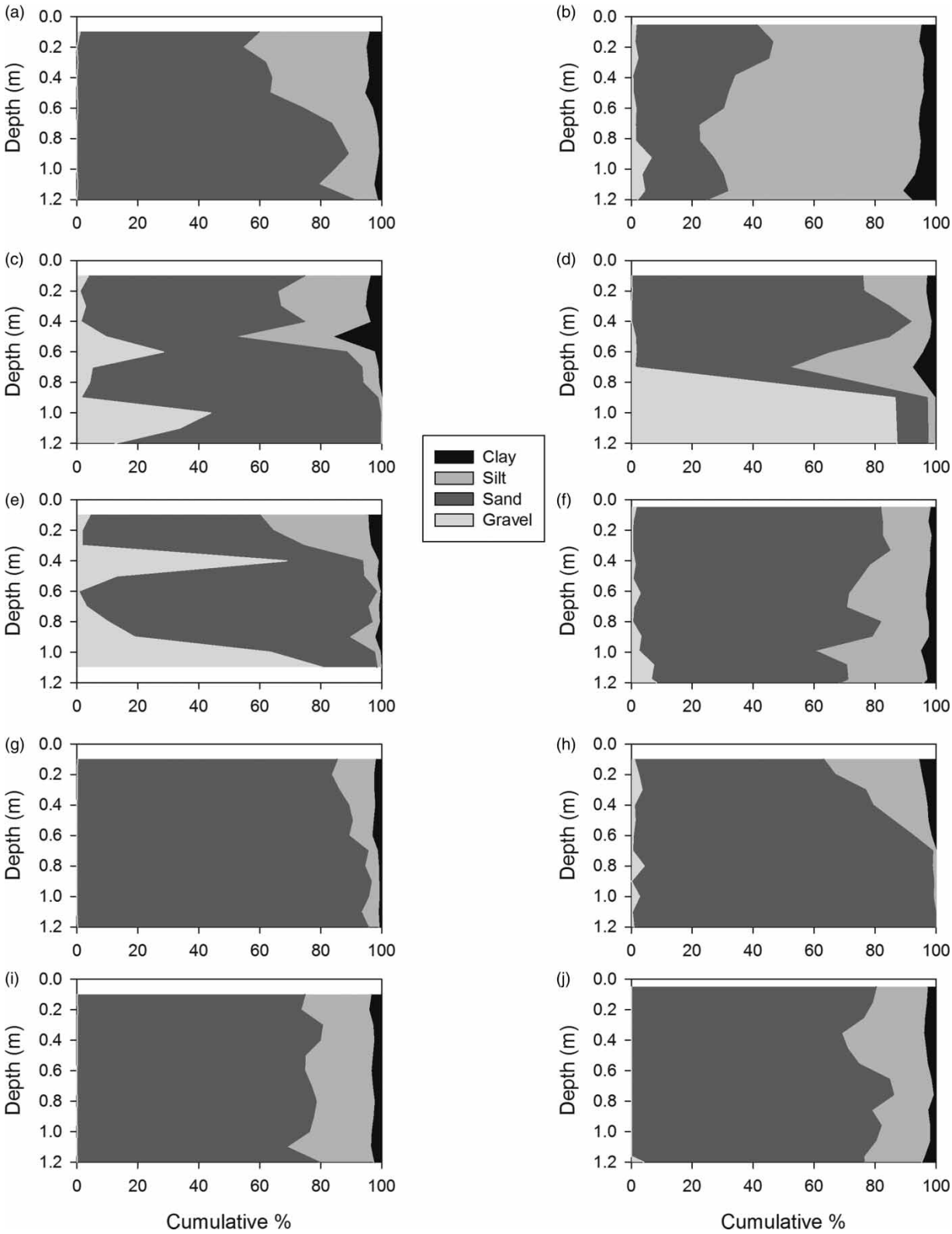

Figure 5 | Vertical profiles of soil texture: (a) OPEN1, (b) OPEN2, (c) MH1, (d) MH2, (e) MH3, (f) YP1, (g) YP2, (h) YP3, (i) OP1 and (j) OP3.

Downloaded from http://iwaponline.com/hr/article-pdf/47/2/390/368866/nh0470390.pdf
by guest

Table 3 | Summary of above-canopy precipitation (P_g), throughfall (*TF*), interception (*I*) and stemflow (*SF*) for the study period, growing season and winter–spring

Site	P_g[a] (mm)	Total *TF*[a] (mm)	Total $TF:P_g$	Growing season P_g or *TF*[b] (mm)	Growing season $TF:P_g$	Winter–spring *TF*[c] (mm)	Winter–spring $TF:P_g$	TF_F (mm)	$TF_F:P_g$	Weighted *TF* (mm)	Weighted $TF:P_g$	*I* (mm)	$I:P_g$	*SF*[d] (mm)	Stand-scale $SF:P_g$	*SF* weighted by 0.2 m focusing zone (mm)	Focusing zone $SF:P_g$
OPEN1	1,239			745		287											
OPEN2	1,205			705		285											
MH1	1,205	944	0.78	516	0.73	260	0.91	1,997	1.66	1,009	0.84	245	0.20	16	0.013	1,657	1.38
MH2	1,205	998	0.83	554	0.79	264	0.93	2,091	1.74	1,051	0.87	186	0.15	21	0.017	1,657	1.38
MH3	1,335	1,090	0.82	659	0.83	254	0.86	2,167	1.62	1,197	0.90	229	0.17	16	0.012	1,657	1.24
YP1	1,239	1,074	0.87	644	0.86	249	0.87					161	0.13	4	0.003	140	0.11
YP2	1,239	1,023	0.83	625	0.84	227	0.79					212	0.17	4	0.003	140	0.11
YP3	1,239	1,074	0.87	671	0.90	227	0.79					159	0.13	6	0.005	140	0.11
OP1	1,199	1,004	0.84	607	0.90	215	0.85					194	0.16	1	0.001	101	0.08
OP3	1,335	1,074	0.80	666	0.84	220	0.75					260	0.19	1	0.001	101	0.08

TF_F is focused *TF* within 0.5 m of MH tree boles and weighted *TF* is the weighted mean of MH *TF* from within and outside the *TF* focusing zone, using representative areas as weighting factors.

[a]Total inputs from both rain and snow for the study period.

[b]Sum of rainfall inputs only for periods June 23, 2009–October 1, 2009 and May 5, 2010–July 12, 2010.

[c]Sum of rainfall and snowfall inputs for period December 5, 2009–May 4, 2010.

[d]Scaled-up from monitored trees using stand basal areas (Table 1). See text for details.

Downloaded from http://iwaponline.com/hr/article-pdf/47/2/390/368866/nh0470390.pdf
by guest

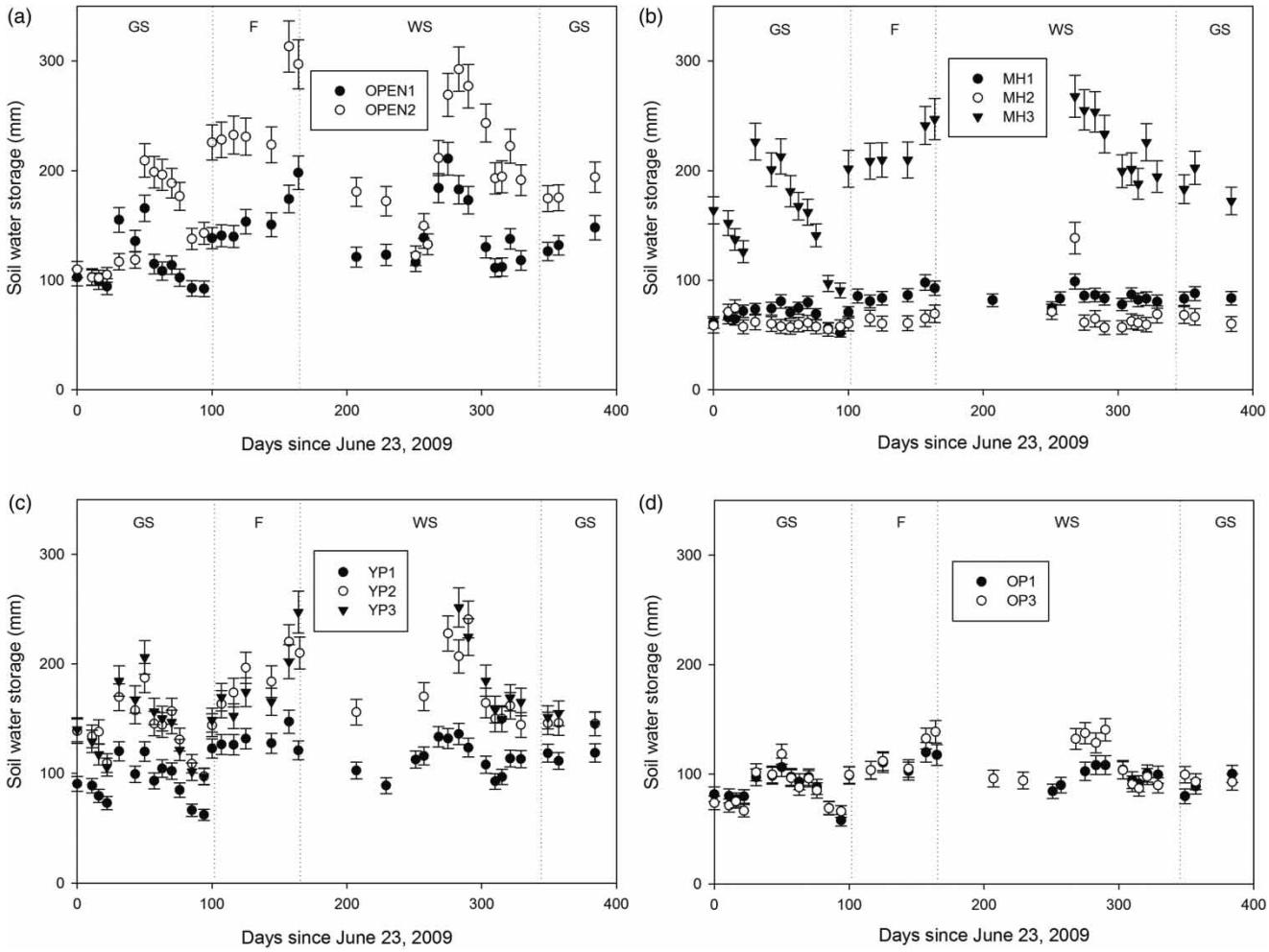

Figure 6 | Changes in soil water storage in the upper 1 m of soil (± estimated error) for the study period: (a) OPEN, (b) MH, (c) YP and (d) OP sites. Vertical dotted lines demarcate study seasons: GS = growing season, F = fall, WS = winter–spring.

Recharge below 1 m depth

Estimated R is summarized in Table 4 and Figure 8. Equivalent annual R (365 days from June 23, 2009) ranged from 88% (MH3) to 94% (OPEN2) of total R given in Figure 8 and Table 4. The difference between maximum (MH3 – 696 mm) and minimum (OP1 – 431 mm) annual R represented ~30% of mean annual precipitation and ~66% of the ~400 mm of mean annual R for the ORM's outcropping sands and gravels (Gerber & Howard 2000, 2002). Larger R for 2009–2010 relative to mean annual R partly reflects above-average study period P_g. Total R showed two distinct groupings: OPEN and MH with R from 594 to 794 mm (49–59% of P_g), and YP and OP with R from 480 to 565 mm (22–39% of P_g). MH sites produced large R ($R_{0.2} > 3{,}200$ mm, $R_{0.2}$:$P_g > 2.5$) close to tree boles, well in excess of R_R. The area 0.2–0.5 m from MH boles produced $R_{0.5} > 2\times$ that of R_R and >130% of P_g, and consideration of these focusing zones increased R for MH stands by 10–18% relative to non-weighted R. Although SF focusing in RP sites enhanced near-bole R, it produced insignificant changes in total R relative to non-weighted R. Consistent inter-site differences in R in a given land cover corresponded to P_g, with OPEN1 > OPEN2, MH3 > MH1 and MH2, and OP3 > OP1 (Figure 8). Nevertheless, error bars often overlapped for R for sites in the same land cover.

There was a general increase in R:P_g from growing season to winter–spring (Table 5), and 55–100% of P_g

Downloaded from http://iwaponline.com/hr/article-pdf/47/2/390/368866/nh0470390.pdf
by guest

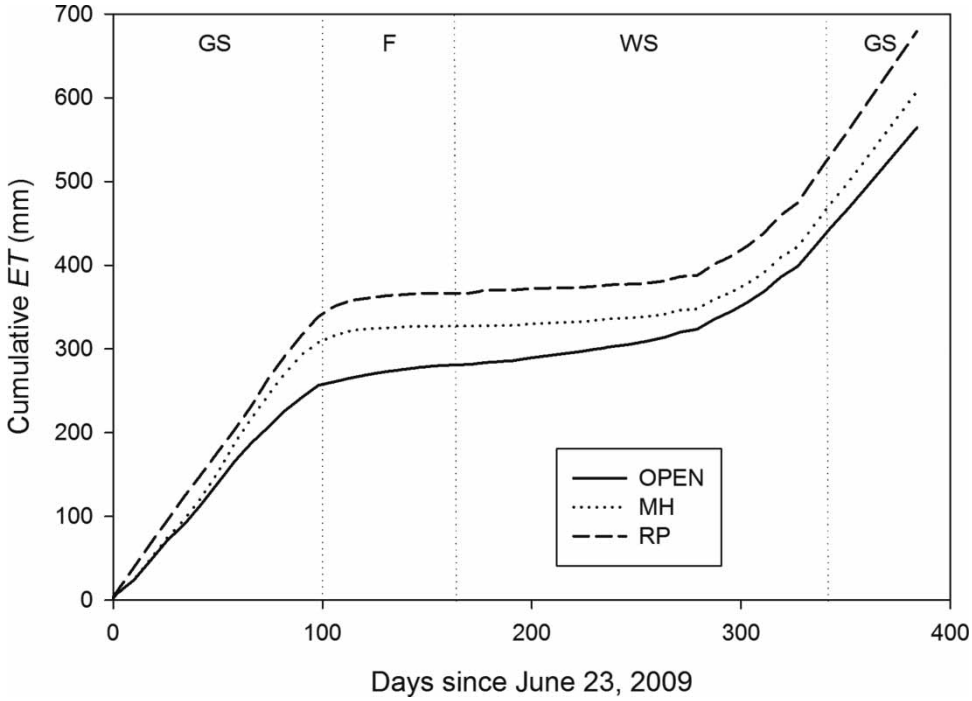

Figure 7 | Cumulative estimated evapotranspiration (*ET*) for the study period for OPEN, MH and RP sites. Vertical dotted lines demarcate study seasons: GS = growing season, F = fall, WS = winter–spring.

Table 4 | Total recharge (*R*) below 1 m depth, *R* by *R* zone ($R_{0.2}$, $R_{0.5}$ *and* R_R) and the fraction of each relative to above-canopy precipitation (P_g) (±estimated error), and the % increase in *R* relative to non-weighted *R*

Site	Total *R* (mm)	Total $R:P_g$	$R_{0.2}$ (mm)	$R_{0.2}:P_g$	$R_{0.5}$ (mm)	$R_{0.5}:P_g$	R_R (mm)	$R_R:P_g$	% change in *R* relative to non-weighted *R*[a]
OPEN1	634 ± 70	0.51 ± 0.06							
OPEN2	594 ± 69	0.49 ± 0.06							
MH1	625 ± 97	0.52 ± 0.08	3,245 ± 663	2.69 ± 0.53	1,587 ± 462	1.32 ± 0.38	534 ± 101	0.44 ± 0.08	14
MH2	630 ± 88	0.52 ± 0.07	3,309 ± 653	2.75 ± 0.54	1,651 ± 489	1.37 ± 0.41	558 ± 90	0.46 ± 0.07	10
MH3	794 ± 93	0.59 ± 0.07	3,389 ± 665	2.54 ± 0.50	1,731 ± 505	1.30 ± 0.38	655 ± 93	0.49 ± 0.07	18
YP1	487 ± 100	0.39 ± 0.08	621 ± 107	0.50 ± 0.09			481 ± 104	0.39 ± 0.08	2
YP2	480 ± 95	0.39 ± 0.08	615 ± 102	0.50 ± 0.08			475 ± 99	0.38 ± 0.08	1
YP3	525 ± 81	0.42 ± 0.07	657 ± 90	0.53 ± 0.09			517 ± 86	0.42 ± 0.07	2
OP1	480 ± 85	0.40 ± 0.07	579 ± 88	0.48 ± 0.07			479 ± 86	0.40 ± 0.07	1
OP3	565 ± 93	0.42 ± 0.07	664 ± 96	0.50 ± 0.07			564 ± 94	0.42 ± 0.07	1

$R_{0.2}$ and $R_{0.5}$ are *R* in the 0.2 m and 0.5 m focusing zones, respectively, and R_R is *R* outside of the focusing zones.
[a]Non-weighted *R* standardizes stemflow (*SF*) by the stand area (see text) and ignores focused throughfall (TF_F), i.e., it assumes spatially uniform *TF* inputs.

recharged during the latter. Growing season *R* and $R:P_g$ at OPEN and MH sites generally exceeded RP values. MH $R:P_g$ ratios were greater relative to OPEN sites, reflecting coarser soil textures at the former (Figure 5). There were no clear distinctions between fall or winter–spring *R* and $R:P_g$ at OPEN-MH relative to RP sites. Sites with marked

Downloaded from http://iwaponline.com/hr/article-pdf/47/2/390/368866/nh0470390.pdf
by guest

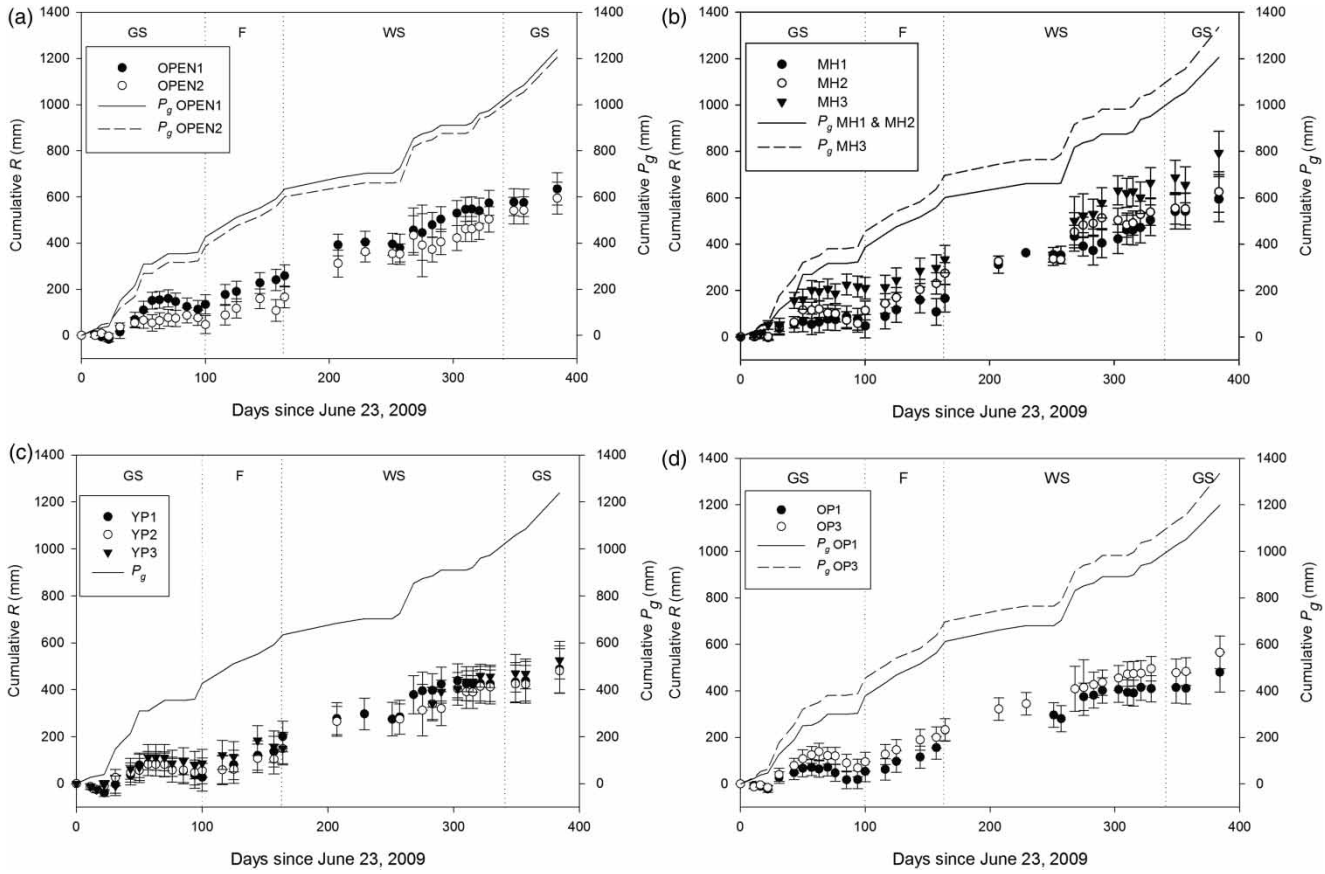

Figure 8 | Cumulative above-canopy precipitation (P_g) and recharge below 1 m depth (R, ± estimated error) for the study period: (a) OPEN, (b) MH, (c) YP and (d) OP. Vertical dotted lines demarcate study seasons: GS = growing season, F = fall, WS = winter–spring.

increases in S_t in fall (OPEN1, OPEN2, MH3, YP2 and YP3, Figure 6) converted less P_g to R relative to sites with little storage change. Conversely, sites with the smallest fall R:P_g values had larger winter–spring R;P_g values, consistent with rapid declines in S_t following snowmelt (Figure 6).

Despite greater total R and R:P_g from OPEN and MH relative to RP sites (Table 4, Figure 8), Z-scores indicated few significant inter-site differences in R (Table 6). OPEN1 had greater R than two RP sites, while MH3 R exceeded that at OPEN and RP sites. There were no significant differences in R or R:P_g between sites in a given land cover, or between YP and OP. Inter-site R differences were largely driven by growing season conditions, with greater R at OPEN1 relative to YP1 and OP1, and at MH3 relative to all RP sites. Greater fall R at sites with little S_t change relative to those with marked S_t increases (Table 5) was often balanced by less R at the former during winter–spring.

DISCUSSION

Hypothesis 1 was partly supported (Table 4) by greater total R from OPEN and MH (594–794 mm) relative to RP stands (480–565 mm), consistent with previous studies. Forests have greater water use (and less R) relative to grasslands (Houghton-Carr *et al.* 2013), and Dripps & Bradbury (2010) found more R from grasslands compared to coniferous forests but greater R from coniferous relative to hardwood forests due to the latter's greater *ET*. However, they did not account for focused *TF* and neglected *SF* when estimating hardwood forest R. Conversion of pine to oak forest increased R by 4.8% largely due to decreased *ET* from the latter (Wattenbach *et al.* 2007), while oak forest R exceeded that from spruce forests approximately 20–25 years following reforestation (Rosenqvist *et al.* 2010). However, the large associated errors meant that only OPEN1 and MH3

Downloaded from http://iwaponline.com/hr/article-pdf/47/2/390/368866/nh0470390.pdf
by guest

Table 5 | Seasonal recharge (R) below 1 m depth and R relative to above-canopy precipitation (P_g) (± estimated error)

Site	Growing season R (mm)	Growing season R:P_g	Fall R (mm)	Fall R:P_g	Winter–spring R (mm)	Winter–spring R:P_g
OPEN1[a]	221 ± 62	0.30 ± 0.08	124 ± 26	0.60 ± 0.13	289 ± 29	1.01 ± 0.10
OPEN2[a]	180 ± 62	0.26 ± 0.09	120 ± 31	0.56 ± 0.14	295 ± 35	1.04 ± 0.12
MH1	249 ± 83	0.35 ± 0.12	160 ± 35	0.74 ± 0.16	217 ± 38	0.76 ± 0.13
MH2	227 ± 71	0.32 ± 0.10	196 ± 28	0.91 ± 0.13	207 ± 32	0.73 ± 0.11
MH3[a]	376 ± 78	0.47 ± 0.10	125 ± 35	0.52 ± 0.15	292 ± 38	0.98 ± 0.13
YP1	89 ± 89	0.12 ± 0.12	173 ± 40	0.84 ± 0.19	224 ± 44	0.78 ± 0.15
YP2[a]	145 ± 84	0.19 ± 0.11	94 ± 38	0.45 ± 0.19	241 ± 42	0.84 ± 0.15
YP3[a]	178 ± 81	0.24 ± 0.11	62 ± 41	0.30 ± 0.20	285 ± 27	0.99 ± 0.10
OP1	143 ± 72	0.21 ± 0.11	178 ± 29	0.76 ± 0.13	159 ± 33	0.55 ± 0.12
OP3	186 ± 79	0.23 ± 0.10	138 ± 33	0.57 ± 0.14	241 ± 37	0.81 ± 0.12

Growing season R is for June 23–October 1, 2009 and May 5–July 12, 2010, fall R is for October 2–December 4, 2009, winter–spring R is for December 5, 2009–May 4, 2010.
[a]Sites exhibiting relatively large variability in soil water storage (Figure 6).

Table 6 | Significant inter-site differences in recharge (R) below 1 m depth for the study period based on Z-scores

Inter-site difference in R	Significance level
OPEN1 > YP2	0.10
OPEN1 > OP1	0.10
MH3 > OPEN1	0.10
MH3 > OPEN2	0.05
MH3 > YP1	0.05
MH3 > YP2	0.05
MH3 > YP3	0.05
MH3 > OP1	0.05
MH3 > OP3	0.05

had total R significantly greater than some (YP2 and OP1 in the case of OPEN1) or all (MH3) of the RP stands (Table 6). Greater total R at MH3 partly resulted from larger P_g and TF inputs (Table 3); nevertheless, inter-site differences in P_g and ET exerted a secondary control on R variations between land covers. Thus, total R was ~800 mm at MH3 and <600 mm at OP3 despite identical P_g (Figure 8(b) and 8(d)), while total period ET was only ~70 mm greater at RP relative to MH stands (Figure 3).

Annual R for land covers was assumed to be primarily influenced by I, with greatest I for mature conifers and least for non-forested areas (Houle *et al.* 1999; Barbier *et al.* 2009). However, R did not follow the hypothesized increase in water inputs along this land cover gradient, with no significant differences in I:P_g ratios between OP, YP and MH stands (Table 3). Thus, while water inputs to the soil were greatest at OPEN sites (1,205–1,239 mm), there was considerable overlap between inputs ($TF + SF$) at MH (960–1,106 mm), YP (1,027–1,080 mm) and OP (1,005–1,075 mm) stands.

This hypothesis also presumed similar ET from the soil across land covers (Sun *et al.* 2008). Study period above-canopy ET was least for OPEN (564 mm) and greatest for RP stands (679 mm), while maximum daily total ET ranged from 3.2 mm d^{-1} (OPEN) to 4.4 mm d^{-1} (MH). Forest ET often exceeds that for grasslands (Eugster & Cattin 2007; Houghton-Carr *et al.* 2013), and greater ET for RP relative to MH stands is consistent with Mackay *et al.* (2002). However, much of the greater RP and MH ET relative to OPEN sites resulted from evaporation of intercepted water. Soil ET when adjusted for I was greatest for OPEN sites (564 mm), intermediate for RP stands (467–550 mm), and least for MH stands (362–427 mm). Total R suggests larger net precipitation inputs more than compensated for greater ET from the soil at OPEN sites.

MH and OPEN R values were similar, partly as a result of less soil ET at MH sites. Greater MH R relative to RP stands also reflects focused SF and TF near MH boles. Many forest recharge studies assume spatially uniform TF (Dripps & Bradbury 2010) and SF (Neary & Gizyn 1994) inputs to the soil, or neglect SF altogether (Dripps & Bradbury 2010). While this is reasonable in RP where SF

Downloaded from http://iwaponline.com/hr/article-pdf/47/2/390/368866/nh0470390.pdf
by guest

contributions to R were negligible (Table 4), MH branch architecture focuses TF and SF towards the bole (Carlyle-Moses & Price 2006; Sato *et al.* 2011; Bialkowski & Buttle 2015). MH TF_F was >2× the average catch of the 10 TF gauges, and MH generated more SF relative to RP stands. MH SF relative to the 0.2 m wide ring around the bole (Table 3) produced SF fluxes $\sim 1.3 \times P_g$. These were less than the focused $SF{:}P_g$ ratio of 2.7 for beech trees (Voigt 1960), which are more efficient SF producers than maple trees (Carlyle-Moses & Price 2006). Nevertheless, focused near-bole TF and SF represent an important R source (Johnson & Lehmann 2006). Although areas for $R_{0.5}$ and $R_{0.2}$ estimations were only ~4–7% and 1–2% of total stand area, respectively, their inclusion increased MH $R{:}P_g$ by 11–18%. This highlights the importance of including focused inputs in R studies in MH forests.

Inability to monitor SF in all stands during winter–spring led to the assumption of negligible SF for this period. While this may be reasonable for RP (Table 3), Herwitz & Levia (1997) and Levia (2004) showed significant winter SF generation in deciduous forests. Inclusion of focused SF during this period would have increased total (Table 4) and winter–spring (Table 5) MH R; however, the increase is of unknown magnitude and needs further study.

Omission of such SF inputs may partly explain why Hypothesis 2 was not supported. There was no consistent difference in R between land covers in fall and winter–spring, despite considerable I_s in RP sites consistent with other findings (Pomeroy *et al.* 1998; Houle *et al.* 1999) and reductions in rainfall I between leaf-on and leaf-off periods for deciduous species (Gerrits *et al.* 2010). Larger peak SWE in OPEN and MH sites relative to RP stands was also expected to enhance R (Komatsu *et al.* 2008; LaMalfa & Ryle 2008); however, consistent differences between land covers were not seen. Differential ability of sites to store and release soil water also contributed to the failure to support Hypothesis 2. Despite similar soil types, sites showed considerable variability in soil texture and hydrological properties (Figures 3, 4 and 5). All access tubes were >1 m from the bole, and observed changes in S_t should reflect a site's soil textural and hydrologic properties rather than focused TF and SF inputs (Buttle *et al.* 2014). Thus, some sites (OPEN1, OPEN2, MH3, YP2, YP3) showed marked increases in fall S_t regardless of land cover, and had relatively less R compared to sites with limited storage response and greater water transmission through the upper 1 m of soil (Table 5). Conversely, the former sites were relatively wetter prior to snowmelt, suggesting greater unsaturated K_H compared to drier sites and more effective transmission of water inputs through the profile. Drainage of soil water supplemented R at these sites, leading to large $R{:}P_g$ ratios (Table 5). Results highlight the importance of considering soil type in land cover comparisons of R, and the potential for inaccurate R estimates using low resolution soils maps (Faust *et al.* 2006; Crosbie *et al.* 2009).

Growing season MH R was ≥ OPEN sites, with no consistent differences between YP and OP stands. Growing season TF and $TF{:}P_g$ were generally smallest (and I was largest) in MH relative to RP stands (Table 3), suggesting that R should be least at MH stands. Minimum $R{:}P_g$ might also be expected to occur at all sites during the growing season due to greater ET during this period (Figure 7; Faust *et al.* 2006; Dripps & Bradbury 2010). Instead, the greatest fraction of total MH R occurred in the growing season relative to fall and winter–spring. This contrasted with OPEN and RP sites (with the exception of OP1) where winter–spring R contributed the greatest portion of total R. This may reflect the wet summer in 2009 and 2010, combined with enhanced MH R through near-bole SF and TF focusing (Table 4). However, the caveat that unmonitored winter–spring SF in MH stands may have increased R during this period must be considered.

Many hardwood-conifer forests in the GF were converted to agriculture in the 19th century, and the pine plantations intended to suppress soil erosion from agricultural fields and reduce downstream flooding are currently managed to promote re-conversion to mixed hardwood stands (Buttle 2011). Annual R during this land cover transition may decline from high values for grasslands (mean annual $R = 575$ mm) to minima under red pine plantations (mean annual $R = 375$ mm), and subsequently increase for mixed hardwoods (mean annual $R = 616$ mm). The shift in R during this land cover change (~200 mm) represents ~20% of annual precipitation and 50% of the ~400 mm of average annual recharge for exposed sand and gravel deposits on the ORM (Gerber & Howard 2000, 2002), with important implications for groundwater resources. This may also be accompanied by a change in the seasonality

Downloaded from http://iwaponline.com/hr/article-pdf/47/2/390/368866/nh0470390.pdf
by guest

of R, with winter–spring dominating annual R for grasslands and red pine plantations, but with growing season R of increasing importance for mixed hardwoods partly as a result of enhanced R due to focused near-bole inputs of TF and SF.

These R values were for level sites, and superimposed on the suggested temporal trajectory of R during land cover change are topographic controls on the spatial pattern and magnitude of R. Depression-focused R in agricultural areas along the ORM's crest can greatly exceed R on level sites (Greenwood & Buttle 2014b), attributed to frozen winter soils and overland flow of spring snowmelt and rainfall to topographic depressions (Hayashi *et al.* 2003). Its apparent absence in RP plantations and mixed hardwood stands likely results from smaller SWCs prior to freeze-up combined with warmer soil. Thus, the magnitude and spatial pattern of R on the permeable soils mantling the ORM's crest may depend on the combined effects of topography and land cover, and merit further study.

CONCLUSIONS

Accuracy of recharge estimates from 1-d water balances such as those used here depends on the exactitude with which other water balance components have been determined (Healy 2010). Nevertheless, recharge values for major land covers in the GF are in the order of the 400 mm of mean annual recharge estimated for outcropping sand and gravel deposits along the ORM's crest. Differences between maximum and minimum recharge for these land covers represent ~30% of mean annual precipitation and up to 66% of mean annual recharge on the ORM's outcropping sands and gravels, and should be considered when evaluating the ORM's water resources. These differences were not simply a function of inter-site contrasts in precipitation or the ability of different forest types to intercept and subsequently evaporate precipitation. Large errors associated with the recharge values complicated efforts to discern differences between land covers in the GF, as did inter-site variations in the ability of nominally similar soil types to store and transmit water. Nevertheless, annual recharge for grasslands and mixed hardwood stands exceeded that from young and old red pine plantations. This suggests that historical land cover changes along this portion of the ORM from mixed hardwood-conifers → agricultural fields → red pine plantations → regenerating mixed hardwoods were accompanied by shifts in annual recharge. Focused throughfall and stemflow inputs near the boles of mixed hardwoods appear to promote differences between land covers in terms of the fraction of total recharge supplied in growing vs. dormant periods, suggesting that changes in the seasonality of recharge may also accompany this land cover transition.

Recharge values reported here are among the first direct estimates for major land covers on the ORM, and highlight the need to consider the role of land cover when assessing spatial variations in recharge along the ORM. They should also assist efforts to model groundwater flow and understand inter-basin differences in streamflow for this key hydrogeologic feature in southern Ontario.

ACKNOWLEDGEMENTS

This work was supported by the Natural Sciences and Engineering Research Council of Canada. We thank the Ganaraska Region Conservation Authority for continued support; Peter Lafleur, Andrew Farnsworth, Clément Le Saux and Alexandra Ryland for their assistance; Ken Hill and Marie and John Toon for access to their property; Qiaozhen Mu (University of Montana) for the MOD16 data; and two anonymous reviewers for comments on an earlier version of this paper.

REFERENCES

Barbier, S., Balandier, P. & Gosselin, F. 2009 Influence of several tree traits on rainfall partitioning in temperate and boreal forests, a review. *Ann. For. Sci.* **66**, 1–11.

Bialkowski, R. 2015 Groundwater Recharge in a Managed Forest on the Oak Ridges Moraine, Southern Ontario. MSc thesis, Environmental and Life Sciences Graduate Program, Trent University, Peterborough, Ontario, p. 178.

Bialkowski, R. & Buttle, J. M. 2015 Stemflow and throughfall contributions to soil water recharge under trees with differing branch architectures. *Hydrol. Proc.* **29**, 4068–4092.

Bryant, M., Bhat, S. & Jacobs, J. 2005 Measurements and modeling of throughfall variability for five forest communities in the southeastern US. *J. Hydrol.* **312**, 95–108.

Downloaded from http://iwaponline.com/hr/article-pdf/47/2/390/368866/nh0470390.pdf
by guest

Buttle, J. M. 2011 Streamflow response to headwater reforestation in the Ganaraska River basin, southern Ontario, Canada. *Hydrol. Proc.* **25**, 3030–3041.

Buttle, J. M. & Farnsworth, A. 2012 Measurement and modeling of canopy water partitioning in a reforested landscape, The Ganaraska Forest, southern Ontario, Canada. *J. Hydrol.* **466–467**, 103–114.

Buttle, J. M., Toye, H., Greenwood, W. & Bialkowski, R. 2014 Growing season stemflow and soil water recharge in a red pine chronosequence on the Oak Ridges Moraine, southern Ontario, Canada. *J. Hydrol.* **517**, 777–790.

Buttle, J. M., Greenwood, W. J. & Gerber, R. E. 2015 Spatiotemporal patterns of baseflow metrics for basins draining the Oak Ridges Moraine, southern Ontario, Canada. *Can. Wat. Resour. J.* **40**, 3–22.

Carlyle-Moses, D. & Price, A. G. 2006 Growing-season stemflow production within a deciduous forest in southern Ontario. *Hydrol. Proc.* **20**, 3651–3663.

Crosbie, R., McCallum, J. & Harrington, G. 2009 Estimation of groundwater recharge and discharge across northern Australia. In: *Proceedings from, 18th World IMACS/ MODSIM Congress*, Cairns, Australia, pp. 13–17.

Dingman, S. L. 2002 *Physical Hydrology*, 2nd edn. Prentice-Hall, Upper Saddle River, NJ, USA, p. 646.

Dripps, W. R. & Bradbury, K. R. 2010 The spatial and temporal variability of groundwater recharge in a forested basin in northern Wisconsin. *Hydrol. Proc.* **24**, 383–392.

Environment Canada 2011 *National Climate Data and Information Archive, Can. Climate Normals 1971–2000, Peterborough A*. http://www.climate.weatheroffice.gc.ca/climate_normals (retrieved 23 August 2011).

Eugster, W. & Cattin, R. 2007 Evapotranspiration and energy flux differences between a forest and a grassland site in the subalpine zone in the Bernese Oberland. *Die Erde* **138**, 333–354.

Farley, K., Jobbagy, E. & Jackson, R. 2005 Effects of afforestation on water yield, a global synthesis with implications for policy. *Global Change Biol.* **11**, 1565–1576.

Faust, A., Ferré, T., Schaap, M. & Hinnell, A. 2006 Can basin-scale recharge be estimated reasonably with water-balance models? *Vadose Zone J.* **5**, 850–855.

Gelfan, A., Pomeroy, J. & Kuchment, L. 2004 Modeling forest cover influences on snow accumulation, sublimation and melt. *J. Hydrometeor.* **5**, 785–803.

Gerber, R. E. & Howard, K. W. F. 2000 Recharge through a regional till aquitard, three-dimensional flow model water balance approach. *Groundwater* **38**, 410–422.

Gerber, R. E. & Howard, K. W. F. 2002 Hydrogeology of the Oak Ridges Moraine aquifer system: implications for protection and management from the Duffins Creek watershed. *Can. J. Earth Sci.* **39**, 1333–1348.

Gerrits, A., Pfister, L. & Savenije, H. 2010 Spatial and temporal variability of canopy and forest floor interception in a beech forest. *Hydrol. Proc.* **24**, 3011–3025.

Greenwood, W. J. & Buttle, J. M. 2014a Effects of reforestation on near-surface saturated hydraulic conductivity in a managed forest landscape, southern Ontario, Canada. *Ecohydrol.* **7**, 45–55.

Greenwood, W. J. & Buttle, J. M. 2014b Snow, soil frost and land cover relationships on the Oak Ridges Moraine, southern Ontario, implications for topographically-focused groundwater recharge. *Proc. Eastern Snow Conf.* **70**, 95–104.

Hayashi, M., van der Kamp, G. & Schmidt, R. 2003 Focused infiltration of snowmelt water in partially frozen soil under small depressions. *J. Hydrol.* **270**, 214–229.

Healy, R. W. 2010 *Estimating Groundwater Recharge*. Cambridge University Press, Cambridge, UK, p. 245.

Herwitz, S. R. & Levia Jr, D. F. 1997 Mid-winter stemflow drainage from bigtooth aspen (*Populus grandidentata* Michx.) in central Massachusetts. *Hydrol. Proc.* **11**, 169–175.

Houghton-Carr, H. A., Boorman, D. B. & Heuser, K. 2013 *Land use, climate change and water availability, Phase 2a. Rapid Evidence Assessment, Results and Synthesis*. Centre for Ecology & Hydrology, Wallingford, UK.

Houle, D., Ouimet, R., Paquin, R. & Laflamme, J. 1999 Interactions of atmospheric deposition with a mixed hardwood and coniferous forest canopy at the Lake Clair Watershed (Duchesnay, Quebec). *Can. J. Forest Res.* **29**, 1944–1957.

Howard, K. W. F., Eyles, N., Smart, P. J., Boyce, J. I., Gerber, R. E., Salvatori, S. L. & Doughty, J. 1995 The Oak Ridges Moraine of southern Ontario, a ground-water resource at risk. *Geosci. Can.* **22**, 101–120.

Johnson, R. 1990 The interception, throughfall and stemflow in a forest in highland Scotland and the comparison with other upland forests in the U.K. *J. Hydrol.* **118**, 281–287.

Johnson, M. & Lehmann, J. 2006 Double-funneling of trees, stemflow and root-induced preferential flow. *Ecosci.* **13**, 324–333.

Komatsu, H., Kume, T. & Otsuki, K. 2008 The effect of converting a native broad-leaved forest to a coniferous plantation forest on annual water yield. A paired-catchment study in northern Japan. *For. Ecol. Manag.* **255**, 880–886.

Ladekarl, U., Rasmussen, K., Christensen, S., Jensen, K. & Hansen, B. 2005 Groundwater recharge and evapotranspiration for two natural ecosystems covered with oak and heather. *J. Hydrol.* **300**, 76–99.

LaMalfa, M. & Ryle, R. 2008 Differential snowpack accumulation and water dynamics in aspen and conifer communities. Implications for water yield and ecosystem function. *Ecosystems* **11**, 569–581.

Le Maitre, D., Scott, D. & Colvin, C. 1999 A review on interactions between vegetation and groundwater. *Water SA* **25**, 137–150.

Levia Jr, D. F. 2004 Differential winter stemflow generation under contrasting storm conditions in a southern New England broad-leaved deciduous forest. *Hydrol. Proc.* **18**, 1105–1112.

Loustau, D., Berbigier, P., Granier, A. & Hadj Moussa, F. 1992 Interception loss, throughfall and stemflow in a maritime pine stand. I. Variability of throughfall and stemflow beneath the pine canopy. *J. Hydrol.* **138**, 449–467.

Downloaded from http://iwaponline.com/hr/article-pdf/47/2/390/368866/nh0470390.pdf
by guest

Mackay, D., Ahl, D., Ewers, B., Gower, S., Burrows, S., Samanta, S. & Davis, J. 2002 Effects of aggregated classifications of forest composition on estimates of evapotranspiration in a northern Wisconsin forest. *Global Change Biol*. **8**, 1253–1265.

Meriano, M. & Eyles, N. 2003 Groundwater flow through Pleistocene glacial deposits in the rapidly urbanizing Rouge River – Highland Creek watershed, City of Scarborough, southern Ontario, Canada. *Hydrogeol. J*. **11**, 288–303.

Mu, Q., Zhao, M. & Running, S. 2011 Improvements to a MODIS global terrestrial evapotranspiration algorithm. *Remote Sens. Environ*. **115**, 1781–1800.

Neary, A. & Gizyn, W. 1994 Throughfall and stemflow chemistry under deciduous and coniferous forest canopies in south-central Ontario. *Can. J. For. Res*. **24**, 1089–1100.

Nosetto, M., Jobbágy, E. & Paruelo, J. 2005 Land-use change and water losses, the case of grassland afforestation across a soil textural gradient in central Argentina. *Global Change Biol*. **11**, 1101–1117.

Pomeroy, J., Parviainen, J., Hedstrom, N. & Gray, D. 1998 Coupled modelling of forest snow interception. *Hydrol. Proc*. **12**, 2317–2337.

Reynolds, W. D. & Elrick, D. E. 1985 In situ measurement of field saturated hydraulic conductivity, sorptivity, and the alpha-parameter using the Guelph permeameter. *Soil Sci*. **140**, 292–302.

Rosenqvist, L., Hansen, K., Vesterdal, L. & van der Salm, C. 2010 Water balance in afforestation chronosequences of common oak and Norway spruce on former arable land in Denmark and southern Sweden. *Agric. Forest Met*. **150**, 196–207.

Sato, A. M., Avelar, A. de S. & Netto, C. 2011 Spatial variability and temporal stability of throughfall in a eucalyptus plantation in the hilly lowlands of southeastern Brazil. *Hydrol. Proc*. **25**, 1910–1923.

Scanlon, B. R., Reedy, R. C., Stonestrom, D. A., Prudic, D. E. & Dennehys, K. F. 2005 Impact of land use and land cover change on groundwater recharge and quality in the southwestern US. *Global Change Biol*. **11**, 1577–1593.

Sun, G., Noormets, A., Chen, J. & McNulty, S. 2008 Evapotranspiration estimates from eddy covariance towers and hydrologic modeling in managed forests in Northern Wisconsin, USA. *Agric. Forest Met*. **148**, 257–267.

Voigt, G. 1960 Distribution of rainfall under forest stands. *For. Sci*. **6**, 2–10.

Vose, J. M., Sun, G., Ford, C. R., Bredemeir, M., Ostsuki, K., Wei, A., Zhang, Z. & Zhang, L. 2011 Forest ecohydrological research in the 21st century, what are the critical needs? *Ecohydrol*. **4**, 146–158.

Wattenbach, M., Zebisch, M., Hattermann, F., Gottschalk, P., Goemann, H., Kreins, P., Badeck, F., Lasch, P., Suckow, F. & Wechsung, F. 2007 Hydrological impact assessment of afforestation and change in tree-species composition – A regional case study for the Federal State of Brandenburg (Germany). *J. Hydrol*. **346**, 1–17.

Winkler, R. & Hays, W. L. 1975 *Statistics, Probability, Inference, and Decision*, 2nd edn. Holt, Rinehart and Winston, New York, USA, 889 pp. +appendices.

Zhang, Y.-K. & Schilling, K. E. 2006 Effects of land cover on water table, soil moisture, evapotranspiration, and groundwater recharge: a field observation and analysis. *J. Hydrol*. **319**, 328–338.

Zhang, L., Dawes, W. & Walker, G. 2001 Response of mean annual evapotranspiration to vegetation changes at catchment scale. *Water Resour. Res*. **37**, 701–708.

First received 23 February 2015; accepted in revised form 26 July 2015. Available online 22 August 2015

Downloaded from http://iwaponline.com/hr/article-pdf/47/2/390/368866/nh0470390.pdf
by guest